Comparative Studies on Optical Biosensors for Detection of Bio-Toxins

Alexei Nabok

Abstract A number of optical bio-sensing methods were reviewed with their principles and main characteristics outlined. The advantages and disadvantages of optical methods were discussed in a view of their application in detection of bio-toxins. A case study presented the comparative analysis of results in detection of mycotoxins obtained with the method of total internal reflection ellipsometry. The future prospects of optical biosensing technologies were discussed with the main focus on development of portable and highly sensitive biosensors suitable for *in-field* analysis.

Keywords Optical biosensors · SPR · Ellipsometry · Interferometry · Planar waveguides · Mycotoxins

1 Introduction: The Role of Optical Methods in Detection of Bio-Toxins

Detection of bio-toxins of different origins (either produced naturally by different bio-organisms or synthetic) is of great interest nowadays for healthcare, environmental safety, and security. Traditional analytical methods, such as chromatography and mass spectroscopy, are quite capable of both identification and quantification of various bio-toxins in very small concentrations down to ppt range. However those laboratory-based, high-tech methods are expensive and require efforts of specially trained personnel, thus leading to long waiting time and high cost of analysis. Traditional bio-sensing approach based on ELISA immunoassay is more affordable though still laboratory-based and require specialised equipment, highly trained technicians, and expensive chemicals; yet the sensitivity of detection is in ppb range at best.

A. Nabok (✉)
Materials and Engineering Research Institute, Sheffield Hallam University, Sheffield S1 1WB, UK
e-mail: A.Nabok@shu.ac.uk

D.P. Nikolelis and G.-P. Nikoleli (eds.), *Biosensors for Security and Bioterrorism Applications*, Advanced Sciences and Technologies for Security Applications,
DOI 10.1007/978-3-319-28926-7_23

These days, the focus of the development of chemical and bio-sensors has shifted towards portable (ideally hand-held) devices suitable for in-field (or point of care) analysis and at the same time highly sensitive and capable of detection of single molecules of analytes of interest. From the point of view of portability and simplicity of design, nothing can be better than electrochemical sensors; that is why electrochemical sensors dominate the bio-sensing market. Their sensitivity is reasonably high though the selectivity is rather poor, so that the identification of analytes is the main problem for electrochemical sensors. The most common sensitive elements in electrochemical sensors are enzymes which are not directly react with bio-toxins but rather inhibited. The identification of toxins is therefore required the use of sensor array approach with quite complex statistical data analysis and thus unreliable outcome. Since most of bio-toxins are rather small molecules, the use of gravimetric sensors, i.e. QCM and SAW sensors, is limited. Optical immuno-sensors are perhaps the most suitable for detection of bio-toxins since they combine high sensitivity of optical transducers with high selectivity of immune reactions.

The main purpose of this work is to compare several optical bio-sensing technologies on their suitability for detection of bio-toxins and to suggest the ways for future development of sensor devices.

2 Review of Existing Optical Bio-Sensing Technologies

Before going into description of different bio-sensing technologies, we have to outline the parameters on which all these methods will be compared. The sensitivity of detection can be defined as $S = \Delta R/\Delta C$, where ΔR is the changes of the sensor response and ΔC is the variation of the analyte concentration. Since the majority of optical bio-sensing methods are based on detection of changes in refractive index in the sensitive molecular layer, without mentioning specific analytes, the sensitivity can be expressed as $S = \Delta R$/RIU (RIU standing for refractive index unity). Very often instead of sensitivity, we tend to quote the low detection limit (LDL) which is defined as minimal concentration of analytes detected. Obviously LDL is inversely proportional to sensitivity, but also depends on signal to noise ratio for the response. The units for LDL could be in molar concentrations (mM, μM, nM, pM, etc.), or weight of analyte per ml of solution (μg/ml, ng/ml, pg/ml, etc.), which are equivalent to ppm, ppb, and ppt, respectively. Other important characteristics are the level of sensor recovery and the characteristic times of response and recovery. These parameters are related to the kinetics of the response and recovery and depend on the adsorption and desorption rates (k_a, and k_d) as well as on their ratios known as association constant ($K_A = k_a/k_d$) and affinity constant $K_D = 1/K_A = k_d/k_a$. The latter two parameters describe well the specificity of binding the molecule of analyte to receptor. For example, in the case of highly specific immune reactions K_A reaches the level of 10^6–10^8 Mol^{-1}.

Optical immuno-sensing technologies can be split into two categories, namely luminescence (fluorescence) sensors and label-free sensors. In the first one, the sensitive elements, such as proteins, antibodies, enzymes, nano-particles are conjugated with the fluorescent labels; binding analyte molecules to such receptors causes luminescence (fluorescence) or it's quenching. As result the response can be easily visualised either by naked eye or with a suitable photodetector. Fluorescence-based sensing technologies are very popular and particularly suitable for high throughput analysis. The example could be the method of ELISA [1] where the immune reaction can be quantified simultaneously in a large number of channels (typically 96). ELISA was established as a standard bio-sensing method in analytical laboratories, and other bio-sensing methods are commonly compared with it. The sensitivity of ELISA is reasonably high, typically below the ng/ml level. The main drawback of this method is the use of expensive chemicals and long time of preparation for analysis; yet it is a laboratory based method not suitable for *in-field* analysis.

The main focus of this review is on label-free optical methods. Majority of these methods are based on the phenomenon of evanescent field or wave which appear as electromagnetic wave propagating along the interface between two materials with different refractive indices when the light enter the material with lower refractive index at total internal reflection condition; the amplitude of evanescent is exponentially decaying away from the interface. Optical waveguides are based on this principle with the light propagating along the material of higher refractive index (core) when sandwiched between materials of lower refractive index (cladding).

The waveguides could be of different geometries from standard cylindrical in optical fibres to rectangular in planar waveguides and optical slabs. There are a number of sensing technologies based on optical fibres with the simplest one having a tip of the optical fibre coated with sensitive material. The intensity of the reflected light carries the information on interaction between the receptor and analyte molecules. Although such sensors are simple and could be handy for remote in-field analysis, the sensitivity of such optical probes is rather poor, typically in ppm range and below.

More advanced optic fibres sensors utilize diffraction gratings written either in the core or cladding resulting in Bragg-Grating (BG) sensors [2] and long period grating (LPG) sensors [3], respectively. These sensors were found application in remote sensing though the sensitivity of detection has never been high. Regenerating of the sensing surface could be another problem which limits their use for detection of bio-toxins. Sensing applications of the waveguides of planar geometry are very promising and will be discussed later.

The phenomenon of surface plasmon resonance (SPR) constitutes the basis of the most popular optical biosensing technology [4]. Surface plasmon resonance takes place in thin metal (Ag, Au, Cu) films (around 40 nm) deposited on glass. In a classical Kretschmann SPR geometry the light is coupled into thin metal film through the prism (Fig. 1a). When the angle of incidence exceeds the critical angle

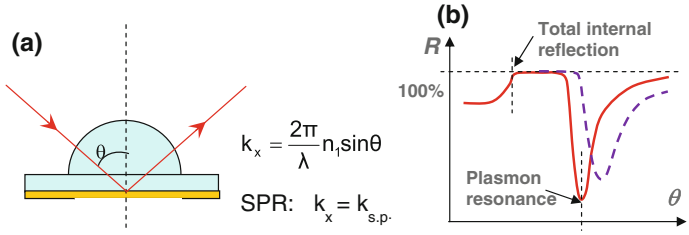

Fig. 1 Kretchamann configuration of SPR (**a**); Typical SPR curve (**b**)

of total internal reflection, almost 100 % of light is reflected and the evanescent wave is propagating along the surface. However, if the k_x vector of the evanescent wave matches the $k_{s.p.}$ vector of surface plasmons in thin metal films, the energy is transferred to plasmons and the reflection intensity drops down.

The dependence of refection intensity against the angle of incidence showed a dip which is called surface plasmon resonance or shortly SRP (Fig. 1b). Since the evanescent wave penetrates into the medium beyond the metal films any molecular adsorption on the surface of metal will cause a shift of SPR peak to high angles, which could be calibrated in terms of molecular concentrations. The effect of SPR is behind the most popular optical bio-sensing technology which was implemented in a large number of commercial instrumentations with BIACORE the most known. The designs are varied: instead of varying the angle of incidence, the wavelength of incident light can be varied which results in a spectroscopic SPR, portable SPR instruments based on this principle were developed. Different types of prisms (triangular, semi-cylindrical) can used for light coupling; instead of a prism, the diffraction grating can be used. The light spot could be widened resulting in SPR imaging instrument [5]. The sensitivity of SPR detection depends very much on the configuration used. The highest sensitivity of 10^{-9} RIU quoted by BIACORE was achieved with the use of special gold plates coated with a 10 nm thick porous layer of dextrane providing the large sensing surface and also containing the reference channel. Otherwise, typical sensitivity of majority of commercial SPR instruments is 3–4 orders of magnitude smaller.

Ellipsometry is another popular optical analytical method based on detection of changes in polarization of light upon its reflection from the investigated surface [4, 6]. The state of polarization of light is fully described by two ellipsometric parameters, namely Ψ and Δ which represent respectively the ratio of amplitudes and the phase shift between p- and s- components of polarized light, $\Psi = A_p/A_s$, $\Delta = \varphi_p - \varphi_s$. Such changes of Ψ and Δ are related to the optical parameters of the reflected surface through Fresnel equations. The presence of any thin film on the reflected surface, which could be a layer of adsorbed molecules, affects the values of Ψ and Δ. By solving Fresnel equations using appropriate software, it is possible to calculate the values of the thickness and refractive index of the adsorbed molecular layer from experimentally recorded values of Ψ and Δ, therefore the ellipsometry can be utilised for detecting different chemical reactions on the

surface, e.g. for sensing. The ellipsometry is a very sensitive analytical tool which is typically used for optical characterisation of various thin films and coatings with the 0.01 nm accuracy of thickness detection and 10^{-5} for refractive index.

Typically ellipsometric instruments comprise the light source, polarizer, compensator, analyser, and photodetector. There are a number of commercial ellipsometric instruments available from basic monochromatic and fixed angle instruments to automated variable-angle, spectroscopic instruments, among them the most known are J.A. Woollam and Jobin Yvon instruments. Despite high sensitivity the ellipsometry in its traditional configuration is hardly used for sensing applications. For sensing purposes, a cell has to be attached to the instrument allowing injection different substances (both gaseous and liquid). The fact that the light travels trough the cell appeared to be the main obstacle for sensing application. The cells can be relatively easily used for gas sensing, but not for sensing in liquids. Different values of refractive index of liquids affect the performance; the liquid medium may also absorb or scatter light. The commercial cells are usually of high volume (tens of millilitres) which is definitely not suitable for bio-sensing which typically operate with microlitres quantities. This problem was overcome about 10 years ago, by combining the ellipsometry and SPR [7, 8] and the new method of total internal reflection ellipsometry (TIRE) was established. The method of TIRE was further developed in the research group of A. Nabok and appeared to be particularly suitable for detection low molecular weight analytes such as mycotoxins [9–13]. The experimental TIRE set-up shown in Fig. 2a is based on a spectroscopic J.A. Woolam M2000 ellipsometric instrument with an addition of a 68° prism in optical contact (via index matching fluid) with gold coated glass slide. A 0.2 ml PTFE cell is sealed against the gold surface via silicon rubber O-ring; the cell has inlet and outlet tubes allowing injection of different solutions. The polarized light is coupled into the gold coated glass slide through the 68° prism which provides total internal reflection conditions on the interface between glass and water. Typical TIRE spectra of Ψ and Δ recorded on bare gold film of 25 nm thick deposited on glass with the cell filled with water are shown in Fig. 2b. As one can see, the spectrum of

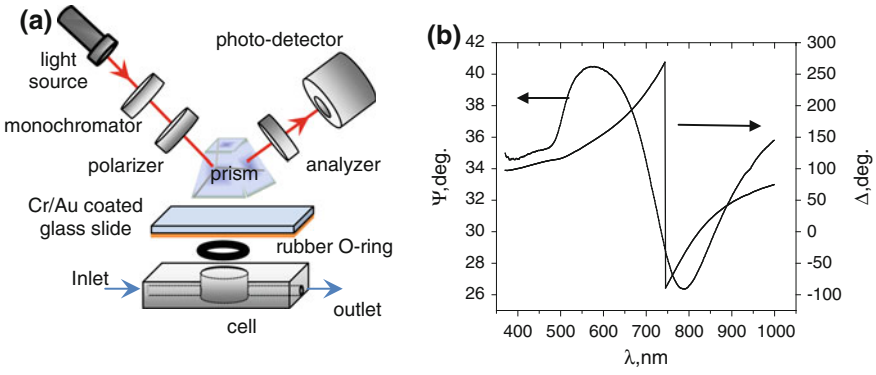

Fig. 2 TIRE experimental set-up (**a**); Typical spectra of Ψ and Δ recorded on bare gold (**b**)

Ψ resembles the classical SRP curve with the maximal signal at about 550 nm wavelength corresponding to total internal reflection conditions and the minimum corresponding to plasmon resonance. It is SPR indeed with the only difference of using a mixture of p- and s- polarised components in contrast to traditional SPR which used p-polarized light only. The spectrum of Δ however represents a new quantity of phase shift between p- and s- components of polarized light, which doesn't exist in SPR. The spectrum of Δ in Fig. 2b shows a phase drop near the resonance, which actually a characteristic of particular instrument used (J.A. Woollam, M200), but it is very sensitive to adsorption of molecules on gold surface and can be calibrated and used as a sensing response. The modelling showed 10 times better sensitivity of the parameter Δ that that of Ψ to small changes of thickness and refractive index in the adsorbed molecular layer [11]. Therefore, for sensing purposes, it better to use the spectra of Δ; the method of TIRE can be called as phase SPR. In both SPR and ellipsometry, the fitting of experimental data to Fresnels equations allows finding the optical parameters of thin molecular films, such as thickness (d) and complex refractive index $N = n - jk$ (where n is refractive index and k is extinction coefficient). However, the limitation of SPR and ellipsometry is that for transparent dielectric films ($k = 0$, $n > 1$) with the thicknesses less than 10 nm it is impossible to find simultaneously the values of d and n. Traditionally in SPR, all changes in the sensing layer are associated with the refractive index, which is fully justified for BIACORE instruments or similar using a porous layer of dextrane with a constant thickness, but it is not always the case. In our experiments using TIRE, for example, it is more logical to "fix" the refractive index and associate all changes with the layer thickness [11]. This is obviously an approximation but it is very close to reality, since majority of biochemicals used have more or less the same refractive index of 1.42 in the visible spectral range [14].

Another very promising method based on evanescent field principle is called optical waveguide lightmode spectroscopy (OWLS) [15–18]. The schematic diagram of OWLS is shown in Fig. 3. It is similar to SPR with the light coupled to a slab waveguide using diffraction grating. The angles of coupling depend on the type of light polarization used p- and s- (often referred in literature as TM and TE,

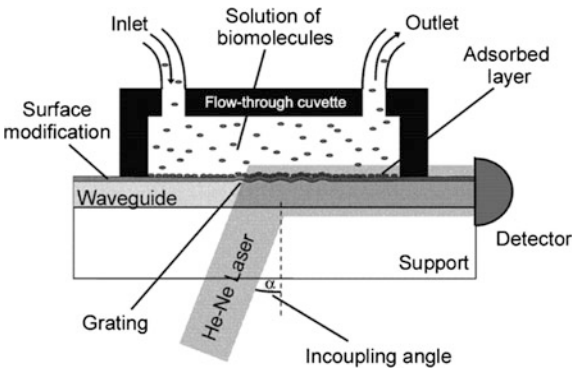

Fig. 3 Schematic diagram of OWLS experimental set-up [15]

respectively). In the method of OWLS, these angles are recorded continuously by rocking the chip by a small angle ±7°, and the two coupling intensity peaks are recoded at the angles of α_s and α_p..

If the adsorption of molecules occurs on the top of the waveguide (a flow injection cell is attached for this purpose) positions of both peaks α_s and α_p shift to higher angles. Because s-polarized light is less affected (as compared to p-polarization) by changes in the adsorbed molecular layer difference between coupling angles $\Delta = \alpha_p - \alpha_p$ can be used as a sensor response and calibrated in concentrations of adsorbed molecules. The sensitivity of OWLS is similar to SPR and is in the range of 10^{-6} RIU. An additional advantage of OWLS, is that the exact solution of mode equations [15, 16] allows the simultaneous determination of n and d of adsorbed molecular layer. A relative disadvantage of OWLS is rather bulky and expensive experimental set-up, so the OWLS is laboratory-based equipment.

It is well known that interferometry is a very sensitive analytical tool in optics; these advantages of interferometry have been exploited in chemical and bio-sensing development. A very successful commercial biosensing instrument was based on dual polarization interferometer (DPI) [19, 20]. The idea of this instrument is quite simple and based on interference of two waves propagating in adjacent slabs and the formation of the interference pattern as shown schematically in Fig. 4. Since the upper waveguiding slab is exposed to the environment, the molecular adsorption affecting the propagating wave causes the shift of the interference pattern which can be quantified in the concentrations of adsorbed molecules. The sensitivity of this method is claimed to be of 10^{-7} RIU which is comparable with the best SPR achievements. The interpretation of the results is not model-dependent (as compared to SPR or ellipsometry), so the outcomes can be easily interpreted as changes in refractive index or thickness, or optical density of molecular layer. The instrument is however quite expensive, bulky, and obviously laboratory based.

Perhaps, the most promising interferomeric scheme for bio-sensing applications is Mach Zehnder interferometer [21], a well-known optoelectronic device used for

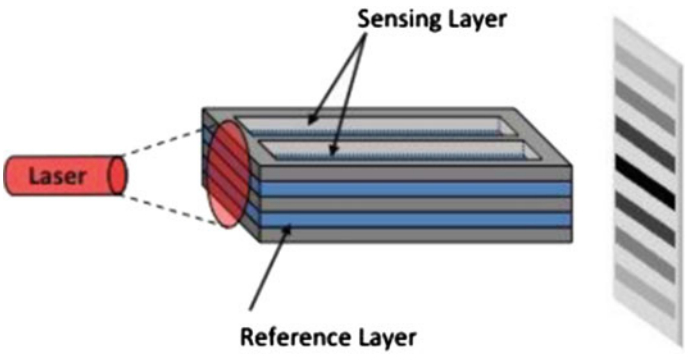

Fig. 4 Schematic diagram of DPI sensor

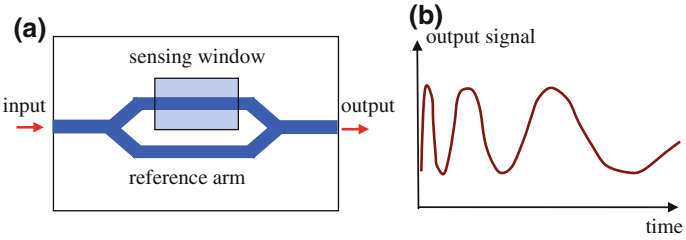

Fig. 5 The scheme of Mach-Zehnder interferometer (**a**); Multiperiodic output signal (**b**)

mixing and modulating optical signals. It based on a planar waveguide splitting into two arms which then merge together again (see Fig. 5a).

An opening in the cladding in one of the arms (called as a sensing window) acts as the sensing element, while the second arm serves as a reference. The output of MZ interferometer shown in Fig. 5b is a multi-periodic signal proportional to the phase shift between the two arms: $R \approx Sin(\varphi_s - \varphi_r)$, where indices s and r stand for "sensing" and "reference" arms. This multi-periodic signal has to be converted to a voltage proportional to the phase shift. For a while, MZ interferometers were bulky optical equipment, typically built on optical benches and used lasers. Relatively recently, miniaturised MZ devices were fabricated commercially using silicon microelectronics technology for telecommunication. Scientist working in the area of chemical and bio-sensing found these devices extremely useful. The technical problems of connecting optical fibres to MZ planar devices were solved successfully using Telecom fabrication facilities.

It was reported recently on the development of commercial multi-channel bio-sensor comprising dozens of MZ interferometers and ring-resonators (another optoelectronic device to be explained later [22]), integrated LED light sources, and micro-fluidic system of liquid sample delivery.

In the last few years, MZ-based biosensors were developed further using a concept of fully integrated MZ-devices based on SiO_2-Si_3N_4-SiO_2 planar waveguide built on Si wafer with two p-n junctions on each end, one acting as an avalanche LED emitting light straight into the waveguide, and another one acting as photo-detector (see the diagram in Fig. 6 [23–25]).

Such design allowed combining all components on the same platform, e.g. silicon wafer, and producing devices by standard microelectronics silicon technology. A large scale EU FP7 collaborative research project has resulted in a range of biosensing chips comprising an array of MZ integrated devices data acquisition electronics and microfluidics. The reported sensitivity of such devices was in the range of 10^{-7}–10^{-9} RIU. Optical ring resonators were mentioned earlier [22]; this is another fruitful biosensing application of optoelectronic devices, e.g. band filter, produced by telecommunication industry. It comprises two planar SiO_2-Si_3N_4-SiO_2 waveguides are placed on each side in an evanescent coupling distance from a ring made of the same waveguiding material. The electromagnetic wave coupled into the ring forms standing waves with characteristic resonances at $\lambda = 2\pi r/n$, where r is the

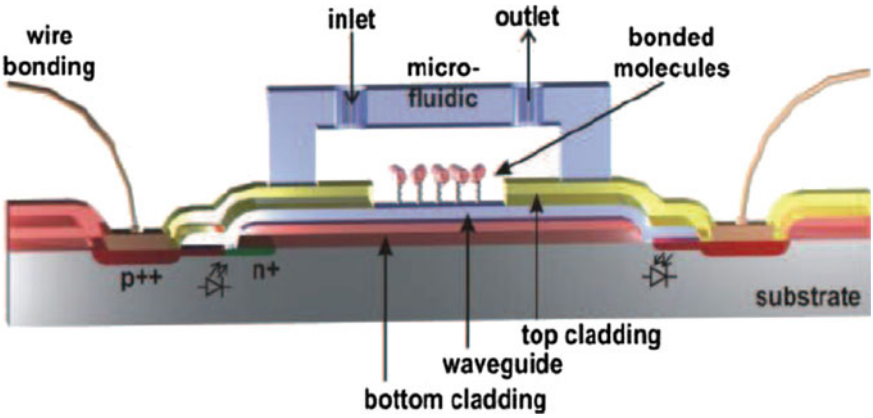

Fig. 6 Fully integrated MZ interferometer sensor [24]

ring radius and n is integer number. Such band-filter devices can be utilized for bio-sensing applications if the sensing window is etched on one of the ring, with another one serving as reference. The sensitivity in the range of 10^{-6} RIU is achievable.

Another very promising biosensing development appeared in the last decade is based on the phenomenon of localized surface plasmon resonance (LSPR). It is quite remarkable that the phenomenon of LSPR has been predicted theoretically by Mie in 1908 [26], then been deserted for nearly a century, and now appeared with a bang due to the rise of material nanotechnologies. The effect of LSPR is caused by oscillations of surface electrons typically in metal nano-structures, such as nano-particles of dimensions comparable with the wavelength of light. Illustration of this phenomenon is given in Fig. 7a. Such oscillations have a characteristic resonance frequency (wavelength) in visible optical range which depends on the type and geometry of metal nano-structures. According to Mie theory, the cross-section

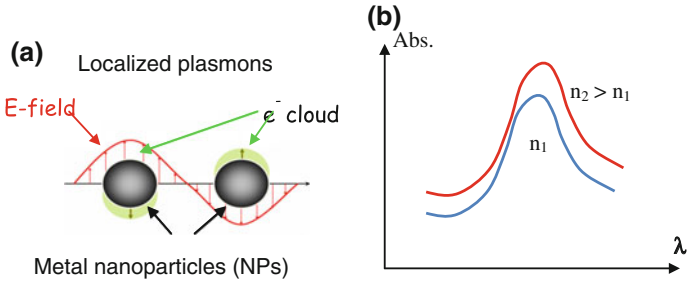

Fig. 7 Interaction of EM wave with surface plasmons in metal nanoparticles (**a**); Spectral shift of LSPR band due to changes in refractive index of the medium (**b**)

of extinction σ_{ext} which sums up the effects of light absorption and scattering on metal spheres of radius r smaller than the wavelength of light is described as [26]:

$$\sigma_{ext} = \frac{12\omega\pi r^3}{c} \frac{\varepsilon_m^{3/2}\varepsilon''(\omega)}{[\varepsilon'(\omega) + 2\varepsilon_m]^2 + \varepsilon''(\omega)^2}$$

where ε_m is the dielectric permittivity of the medium; ε' and ε'' are, respectively, the real and imaginary parts of the dielectric permittivity of metal particles which depend on the circular frequency (ω) of electromagnetic wave. The resonance conditions are achieved when $\varepsilon'(\omega) = -2\varepsilon_m$.

The effect of LSPR is easily detectable using standard spectro-photometry, and LSPR spectra are shown schematically in Fig. 7b. The position and the shape of the LSPR band strongly depend on the refractive index of the surrounding medium, as it obvious from Mie formula. As has been shown more precisely in [27] the refractive index of a medium (n_m) causes the shift of the LSPR peak (λ_{LSPR}) to longer wavelengths in respect to the plasmon peak in bulk material (λ_0): $\lambda_{LSPR} = \lambda_0\sqrt{2n_m^2 + 1}$. This constitutes the main principle of LSPR-based sensors; the molecules adsorbed on the surface of metal nanostructures alter the local refractive index in the vicinity of metal nano-particles thus causing the changes of the absorption band which then can be quantified and calibrated against the concentration of the adsorbed molecules.

The practicality of the LSPR is largely related to the type of metal nano-structures and technology of their fabrications. First of all, metals must be highly conductive which gives an obvious choice of Au, Ag, Cu, etc. Among those metals, gold is the most popular since it combines high conductivity with chemical inertness and well-developed thiol chemistry of its surface modification for immobilization of proteins. Historically, gold nano-particles were perhaps the first type of nano-structures used for LSPR sensing applications [28]. There are a number of well-established recipes of fabrication of gold nano-particles which researches can easily reproduce in the lab to make gold-nanoparticles of particular sizes. Also, nano-particles of gold (as well as some other metals) of various sizes are commercially available these days.

The range of nano-structure types and the methods of their formation is vast and apart from nano-particles included various nano-structures such as nano-rods [29], nano-islands [30], and nano-holes [31]. The variety of metal-nanostructures can be split into two categories: organized and random nanostructures. Random nano-structures are usually self-assembled and thus have irregular shapes and sizes and random spatial arrangement, while organized nano-structures are usually produced by nano-lithography, i.e. electron beam lithography or UV interference lithography [32].

A very smart and elegant method of producing metal nano-structures is the micro-sphere lithography [33]. In this classical work metal (silver) was electro-deposited through the gaps in a monolayer of closely packed polysterene spheres, and the resulted triangular nano-islands arranged in hexagonal 2D lattice were revealed after removing microspheres (Fig. 8).

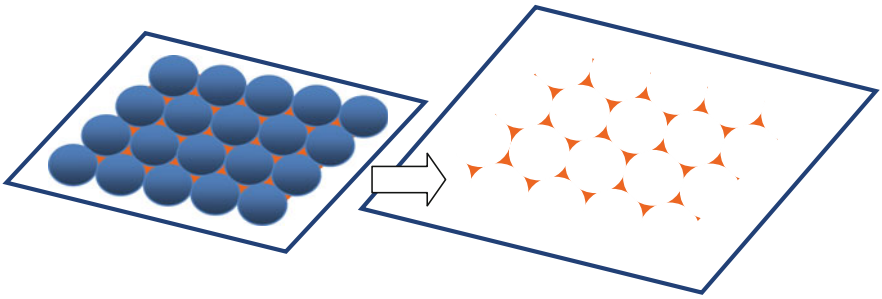

Fig. 8 Formation of metal nanostructures by microsphere lithography [33]

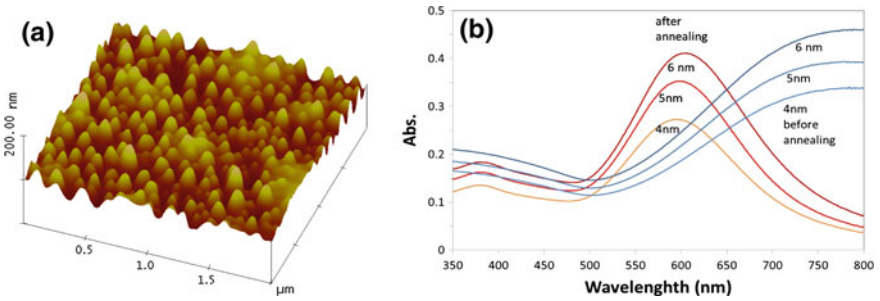

Fig. 9 AFM image of 4 nm Au film thermally evaporated on glass (**a**); UV-vis absorption spectra of thin Cr/Au films before and after annealing (**b**)

However, the simplest technology of making metal nano-structures is annealing of thin metal films. Figure 9a shows the formation of nano-islands structure after annealing at 480 °C for 1–2 h a 4 nm thick gold film thermally evaporated on glass (2 nm layer of Cr was evaporated first to provide good adhesion). The respective absorption spectra in Fig. 9b show the transition from a classical Drude dispersion to a pronounced LSPR band at about 560 nm as a result of annealing.

The formation of nano-islands by de-wetting of continuous thin metal films at high temperatures has been studied systematically by Rubinstein and his colleagues. The refractive index sensitivity depends on the thickness and the size of metal nano-structures, and typically found to be in the range of 50–150 nm/RIU [34].

The spectra of alongated nanoparticles or nano-structures of more complex geometries revealed multiple LSPR peaks which still can be explained using classical electrodynamic theory [35]. For example, the rectangular particles of different aspect ratio yield three LSP peaks which correspond to depolarization factors along all three dimensions, length, width, and height [36]. Increasing of the aspect ratio results in further red shift of the third peak (at the longest wavelength) while the first two peaks remained the same. A very high sensitivity of LSPR down to single molecule level was claimed. This is however a trivial fact considering

small dimensions of nano-particles which can indeed adsorb a single molecule of analyte. Accumulative effect of all nano-particles, yield rather modes sensitivity in the range of … which is suitable for detection of large molecules such as proteins, but not sufficient for detection of bio-toxins of low molecular weight.

The research in optical properties of metals nano-structures revealed the phenomenon of surface enhanced Raman scattering (SERS) which may revolutionise chemical and bio-sensing. The SERS is know long time ago as the method of substantial enhancement of sensitivity of Raman spectroscopy using rough surfaces [37] due to scattering of the electromagnetic waves and the associated local enhancement of electric field. Certain types of metal nanostructures, such as pointed towards each other triangles formed by micro-sphere lithography, appeared to show a huge enhancement of Raman signal up to 10^9 times [37]. The reason behind such enhancement is the presence of so-called "hot spots" having much large values of electric field near the sharp edges. Our recent experiments with pointed gold nanostructures obtained by interference lithography revealed the 6 orders of magnitude enhancement of some vibration bands in adsorbed metal-phthalocyanine molecules [32]. The effect of SERS can be particularly useful for chemical sensing. Bio-toxins of different types can be identified by their characteristic vibration-spectra signatures; the sensitivity of detection could truly go to a single molecule level. However, SERS usually works in a very narrow spectral range and can enhance only particular vibration bands. That is why, researchers use dye molecules acting as Raman labels. Recent development in SERS sensing showed a possibility of "broad-band" SERS which provide large enhancement of 10^5–10^6 in a wide spectra range covering practically all IR spectra [38]. This was achieved using a specially designed and fabricated with electron beam lithography SERS nano-antenna having multiple hot-spots of different resonant frequencies.

3 Case Study: Detection of Bio-Toxins Using TIRE

The main problem of optical detection of bio-toxins is their relatively small molecular weight, so that only the most sensitive analytical tools can be utilised for this task. The detection of mycotoxins was (and still is) a very important problem related to food and feed safety, as well as to security. There are huge varieties of fungi releasing different mycotoxins some of which are toxic, carcinogenic, endocrine disruptive agents, so that the contamination of agriculture products with mycotoxins as well as derivative food and feed constitute a real danger. The above hazardous properties together with the simplicity of mycotoxins production make them listed as substances of potential terrorism activities and biological warfare. In this research we focused on detection of three mycotoxins, namely T2, zearalenone, and aflatoxin B1 in the immunoassays with respective antibodies. Initially tried method of SPR appeared to be not sensitive enough for detection of mycotoxins, therefore the recently developed method of TIRE was selected as the main biosensing technique.

For immobilization of antibodies on the surface of gold, the method of electrostatic deposition, which has been developed in our research group, was used [4]. Standard microscopic glass slides were coated with 25 nm thick gold film with a 3 nm underlayer of chromium providing good adhesion of gold to glass. In order to increase the negative surface charge, gold coated slides were treated overnight in 100 mM solution of mercapto-ethylene-sulfonate sodium salt. The following depositions steps were carried out in the reaction cell of TIRE experimental set-up shown in Fig. 2. The spectra of Ψ and Δ were recorded in the same standard Tris-HCl buffer solution (pH 7.5) after each adsorption or binding step. In addition, the kinetics of molecular adsorption or binding has been studied by recording Ψ and Δ spectra many times after a certain time interval, and then plotting time dependences of Ψ and Δ at particular wavelengths. The first step was the deposition of polycationic layer of poly-allylamine hydrochloride (PAH) from its 1 mg/ml solution in deionised water. Then a layer of protein A was electrostatically adsorbed from its solution in Tris-HCl buffer, pH 7.5–8. Then antibodies to respective mycotoxins were immobilized on the surface. IgG based antibodies having a binding site to protein A in the second domain were oriented on the surface with the fab-fragments pointing towards the solution. Immune binding of the mentioned above mycotoxins to their specific antibodies immobilised on the surface was carried out by consecutive injection of small amounts of toxin into the cell starting form the smallest concentrations.

In the example of T2 immunoassay, the kinetics of the immune binding of T2 molecules to specific antibodies was studied by TIRE dynamic scans during injection of T2 into the cell. The kinetics data analysis protocol was based on differential equation of adsorption on single binding cites [11–13]. The experimental time dependencies of Ψ or Δ were fitted to exponential function and the time constant (τ) was evaluated. Such procedure was repeated for different concentrations (C) of mycotoxins, and a linear dependence of $1/\tau = k_a C + k_d$ versus C was plotted. The rates of adsorption (k_a) and desorption (k_d) were found, respectively, as the gradient and intercept of this dependence. Then the value of the association constant can be found as $K_A = k_a/k_d$. The obtained values of K_A for all three mycotoxins studied were in the range of 10^7 Mol^{-1} which is typical for highly specific immune binding between mycotoxins and respective antibodies.

Typical spectra of Δ recorded after each adsorption (binding) step shown in Fig. 10 demonstrate the "red" spectral shift which is proportional to the size (or mass) of the adsorbed molecules. For sensing purposes, it would be sufficient to just calibrate the shift of Δ spectra in concentrations of mycotoxins. The detection limit for mycotoxins in the range of 0.1 ng/ml is very good for direct immunoassay. However, we were also interested in the physical meaning of the response, so that the fitting of TIRE data was carried out using an upside-down four-layer ellipsometric model consisting of BK7 glass (ambient), Cr/Au film, molecular layer, and water (substrate) [11].

Dispersions functions for n and k for all materials used were taken from J.A. Woollam database. The effective thickness (d) and dispersions of $n(\lambda)$ and $k(\lambda)$ for Cr/Au layer were found first from TIRE spectra recorded on bare gold layer, then

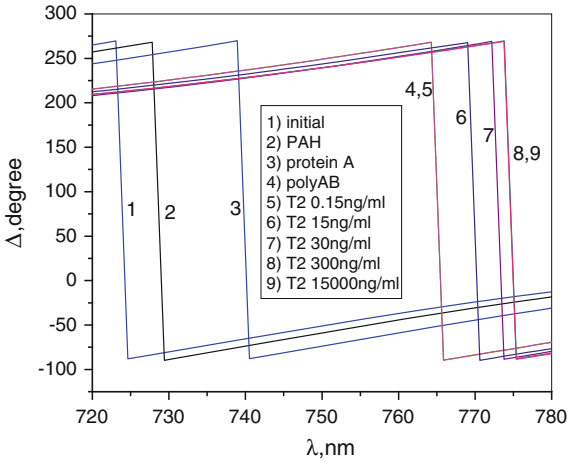

Fig. 10 TIRE spectra of D recorded on after each adsorption (binding) step [10]

these parameters were kept fixed at further fittings. The molecular layer was modelled by Cauchy layer $n = A + B/\lambda^2 + C/\lambda^4$ where the parameters of $A = 1.39$, $B = 0.01$, and $C = 0$ were fixed giving the value of $n = 1.42$ at 633 nm, also $k = 0$. Therefore all changes taken place in the molecular layer were associated with the thickness d.

The resulted data were presented in Fig. 11 as calibration curves, i.e. dependences of the thickness increment vs concentration of mycotoxins, for all three mycotoxins studied. As one can see, all mycotoxins show similar sigmoid type calibrations typical for immune reactions with LDL of 0.1 ng/ml. 10 times lower LDL (0.01 ng/ml) was achieved for detection of Zearalenone using competitive immunoassay [12]. It was interesting to note that the thickness increments of 4.5,

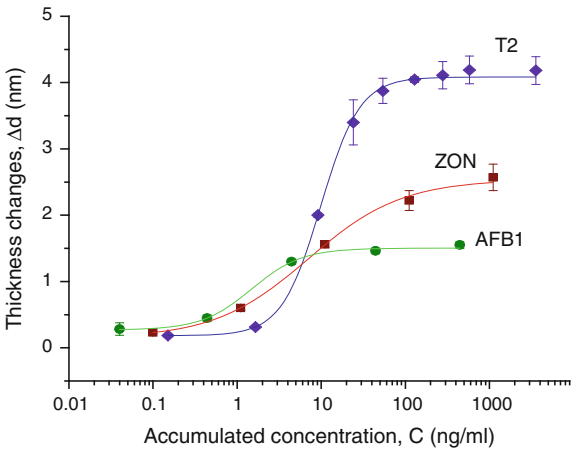

Fig. 11 The TIRE calibration curves for three mycotoxins studied

2.5, and 1.5 nm for T2, ZON, and AFT, respectively, are larger than actual dimensions of corresponding mycotoxins, especially considering that the obtained thickness values are effective because of signal averaging over a large area (15 mm^2) of a light beam spot. This could be a result of aggregation of hydrophobic mycotoxin molecules in water solutions.

The concept of molecular aggregation has been proved when studying immune binding of nonylphenol to respective monoclonal antibodies using a similar TIRE experimental protocol [39]. It appeared that the maximal thickness increment in calibration curve reached 25 nm, a huge thickness nearly 20 times larger than the length of nonylphenol molecule. Also a substantial mass gain was recorded with QCM, and the formation of large aggregates was observed with AFM. The experimental results obtained supported the idea of the formation of micelles of amphiphilic nonylphenol molecules when the initial stock solution of nonylphenol in acetonitrile was diluted with water. Such large aggregates can still bind specifically to antibodies with the association constant in the range of 10^6 Mol^{-1}; the modelling showed that the nonylphenol micelles having rather a "flat pancake" shape can bind to several anaibodies simultaneously [40]. Similarly, specific binding of molecular aggregates (though of much smaller sizes) to antibodies may take place in the case of hydrophobic mycotoxin molecules. This may give an additional boost in sensitivity as compared to adsorption of single molecules.

The method of TIRE has been successfully utilized for detection of some other bio-toxins, namely herbicides pesticides simazine and atrazine [9] and microcystin LR released by bacterial algae [41]. Therefore, the method of TIRE is particularly attractive for detection of low molecular weight analytes as most of bio-toxins are. The sensitivity in sub-ppb level is achievable with TIRE.

4 Conclusions and Future Prospects for Bio-Toxins' Sensor Development

The main outcome of the analysis of literature as well as from our own experience was that the interferometric sensors offer much lower LDL for bio-toxins in pMol or even in fMol range, three orders of magnitude better as compared to more traditional optical methods of SPR, OWLS, TIRE. This is because of multiple reflections of light in planar waveguide structures having large differences between the core and cladding. Scaling down sensing devices to a hand-held type is another major issue in sensing development. From that point of view, MZ interferometers and ring resonators together with microfluidic system produced with the use of advance telecommunication technological facilities is very promising. Fully integrated MZ devices recently developed within EU FP7 project are perhaps the most attractive from the point of view of miniaturization. Such devices can be integrated together with microfluidic and signal acquisition system into a single silicon

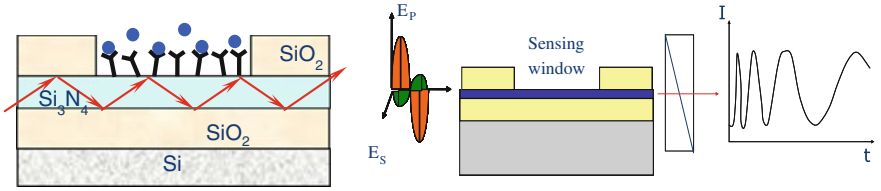

Fig. 12 The design and experimental set-up of planar waveguide-based PPI sensor

chip. This may result in development of highly sensitive and portable (mobile phone size) sensors for *in-field* analysis with the grate benefits for agriculture, food industry, medical testing, environmental safety, and security.

In addition to existing planar waveguide designs, we would like to develop (within ongoing NATO SPS project) a novel type of interferometric sensor devices based the principle of planar polarization interferometry (PPI) shown in Fig. 12. A polarized light coupled into the waveguide experiences a large number of reflections (up to 5000 per mm) causing a substantial phase shift between *p*- and *s*-polarization components (the latter one less affected by the medium serves as a reference). The resulted output signal is multi-periodic similarly to MZ interferometer.

Preliminary experiments [42] and modelling [12] showed a possibility of sensitivity enhancement of minimum 1000 times as compared to the TIRE method, so that the LDL of detection bio-toxins may go down to pg/ml or even lower.

Acknowledgment This work was financially supported by NATO project, SPS(NUKR.SFPP 984637).

References

1. Lequin R M (2005) Enzyme Immunoassay (EIA)/Enzyme-Linked Immunosorbent Assay (ELISA). Clin Chem 51(12):2415–2418
2. Rao Y J (1999) Recent progress in applications in fibre Bragg grating sensors. Opt Lasers Eng 31:297–324
3. James S W, Tatam R P (2003) Optical fibre long-period grating sensors: characteristics and application. Meas Sci Technol 14:R49–R61
4. Nabok A (2005) Organic and inorganic nanostructures. Artech House, Boston
5. Brockman J M, Nelson B P, Corn R M (2000) Surface plasmon imaging of ultrathin organic films. Ann Rev Phys Chem 51:41–63
6. Azzam R M A, Bashara N M (1992) Ellipsometry and polarized light. North Holland, Amsterdam
7. Westphal P, Bornmann A (2002) Biomolecular detection by surface plasmon enhanced ellipsometry. Sens Actuators B 84:278–282
8. Arwin H, Poksinski M, Johansen K (2004) Total internal reflection ellipsometry: principles and applications. Appl Opt 43:3028–3036

9. Nabok A, Tsargorodskaya A, Hassan A K, Starodub N F (2005) Total internal reflection ellipsometry and SPR detection of low molecular weight environmental toxins. Appl Surf Sci 246(4):381–386
10. Nabok A, Tsargorodskaya A, Holloway A, Starodub N F, Gojster O (2007) Registration of T-2 mycotoxin with total internal reflection ellipsometry and QCM impedance methods. Biosens Bioelectron 22(6):885–890
11. Nabok A, Tsargorodskaya A (2008) The method of total internal reflection ellipsometry for thin film characterisation and sensing. Thin Solid Films 516(24):8993–9001
12. Nabok A, Tsargorodskaya A, Mustafa M K, Szekacs I, Starodub N F, Szekacs A (2011) Detection of low molecular weight toxins using optical phase detection techniques. Sens Actuators B Chem 154(2):232–237
13. Nabok A, Mustafa M K, Tsargorodskaya A, Starodub N F (2011) Detection of aflatoxin B1 with a label free ellipsometry immunosensor. BioNanoScience 1(1):38–45
14. Székács A, Adányi N, Székács I, Majer-Baranyi K, Szendrő I (2009) Optical waveguide lightmode spectroscopy immunosensors for environmental monitoring. Appl Opt 48:B151–B158
15. Voros J, Ramsden J J, Gsucs G, Szendro I, De Paul S M, Textor M, Spenser N D (2002) Optical grating couple biosensor. Biomaterials 23:3699–3710
16. Voros J (2004) The density and refractive index od adsorbing protein layers. Biophys J 87:553–561
17. Label-free immunosensor for herbicide trifluralin detection, OWLS Application notes No-002, http://www.OWLS-sensors.com
18. Label-free immunosensor for Aflatoxin B1, OWLS Application notes No-006. http://www.OWLS-sensors.com
19. Cross G, Reeves A A, Brand S, Popplewell J F, Peel L L, Swann M J, Freeman N J (2003) A new quantitative optical biosensor for protein characterisation. Biosens Bioelectron 19 (4):383–390
20. Cross G, Reeves A A, Brand S, Swann M J, Peel L L, Freeman N J, Lu J R (2004) The metrics of surface adsorbed small molecules on the Yung's fringe dual-slab waveguide interferometer. J Phys D Appl Phys 37:74–80
21. Luff B J, Wikinson J S, Piehler J, Hollenbach U, Ingenhoff J, Fabricius N (1998) Integrated optical Mach-Zehnder biosensor. J Lightwave Technol 16(4):583–592
22. Sun Y, Fan X (2011) Optical ring resonators for biochemical and chemical sensing. Anal Bioanal Chem 399:205–211
23. Misiakos K, Kakabakos S E, Petrou P S, Ruf H H (2004) A monolithic silicon optoelectronic transducer as a real-time affinity biosensor. Anal Chem 76:1366–1373
24. Kitsara M, Misiakos K, Raptis I, Makarona E (2010) Integrated optical frequency-resolved Mach-Zehnder interferometers for label-free affinity sensing. Opt Express 18:8193–8206
25. Misiakos K, Raptis I, Makarona E, Botsialas A, Salapatas A, Oikonomou P, Psarouli A, Petrou PS, Kakabakos SE, Tukkiniemi K, Sopanen M, Jobst G (2014) All silicon monolithic Mach-Zehnder interferometer as a refractive index and bio-chemical sensor. Opt Express 22 (22):26803–26813
26. Mie G (1908) Beitge zur optic trüber medien, speziell kolloidaler metallösungen. Ann Phys 330(3):377–445
27. Hong Y, Huh Y-M, Yoon D S, Yang J (2012) Nanobiosensors based on localized surface plasmon resonance for biomarker detection, Hindawi Publishing Co. J Nanomater 759830. doi:10.1155/2012/759830
28. Zhao J, Zhang X, Yonzon C R, Haes A J, Van Duyne R P (2006) Localized surface plasmon resonance biosensors. Nanomedicine 1(2):1029–1034
29. Lee K-S, El-Sayed M (2005) Dependence of the enhanced optical scattering efficiency relative to that of absorption for gold metal nanorods on aspect ratio, size, and- cup shape, and medium refractive index. J Phys Chem 109(43):20331–20338
30. Vaskevich A, Rubistein I (2013) Nanoplasmonic sensors. Springer, Integrated Analytical System, pp 333–368

31. Jonsson M P, Dahlin A B, Jonsson P, Hook F (2008) Nanoplasmonic biosensing with focus on short-range ordered nanoholes in thin metal films. Biointerphases. J Biomater Biol Interphases 3:FD30. doi:10.1116/1.3027483
32. Tsargorodska A, El Zubir O, Darroch B, Cartron M L, Basova T, Hunter C N, Nabok A V, Leggett G J (2014) Fast, simple, combinatorial routes to the fabrication of reusable, plasmonically active gold nanostructures by interferometric lithography of self- assembled monolayers. ACS Nano 8(8):7858–7869
33. Jensen T R, Duval M L, Kelly K L, Lazarides A A, Schatz G C, Van Duyne R P (1999) Single nanosphere lithography: effect of external dielectric medium on the surface plasmon resonance spectrum of a periodic array of silver nanoparticles. J Phys Chem B 103(45):9846–9853
34. Karakouz T, Holder D, Goomanovsky M, Vaskevich A, Rubinstein I (2009) Morphology and refractive index sensitivity of gold island films. Chem Mater 21:5875–5885
35. Gans R (1912) Ann Phys (Weinheim, Ger.) 103:9846
36. Petryaeva E, Krull U J (2011) Localized surface plasmon resonance: nanostructures, bioassays and siosensing—a review. Anal Chim Acta 706:8–24
37. Larkin P J (2005) IR and Raman Spectroscopy. Jones and Bartlett Publishers Inc, Burlington
38. Aouani H, Rahmani M, Šípová H, Torres V, Hegnerová K, Beruete M, Homola J, Hong M, Navarro-Cía M, Maier S A (2013) Plasmonic nanoantennas for multispectral surface-enhanced spectroscopies. J Phys Chem C 117:18620–18626
39. Nabok A, Tsargorodskaya A, Holloway A, Starodub NF, Demchenko A (2007) Specific binding of large aggregates of amphiphilic molecules to respective antibodies. Langmuir 23 (16):8485–8490
40. Lishchuk S, Tsargorodskaya A, Nabok A (2008) The model of alkylphenol micelles bound to respective antibodies on the solid surface. Colloids Surf A 324:117–121
41. Al-Ammar R, Nabok A, Hashim A, Smith T (2015) Microcystin-LR produced by bacterialalgae: Optical detection and purification of contaminated substances. Sens Actuators B Chem 209:1070–1076
42. Starodub N F, Nabok A V, Starodub V M, Ray A K, Hassan A K (2001) Immobilisation of biocomponents for immune optical sensors. Ukrainian Bio Chem J 73:55–64